DRAFT VERSION FEBRUARY 20, 2017
Preprint typeset using LaTeX style emulateapj v. 12/16/11

arXiv:1702.05143v1 [astro-ph.HE] 16 Feb 2017

SEARCHING FOR THE EXPELLED HYDROGEN ENVELOPE IN TYPE I SUPERNOVAE VIA LATE-TIME Hα EMISSION

J. VINKO[1,2,3], D. POOLEY[4], J. M. SILVERMAN[1], J. C. WHEELER[1], T. SZALAI[3], P. KELLY[5], P. MACQUEEN[1], G. H. MARION[1] AND K. SÁRNECZKY[2]

Draft version February 20, 2017

ABSTRACT

We report the first results from our long-term observational survey aimed at discovering late-time interaction between the ejecta of hydrogen-poor Type I supernovae and the hydrogen-rich envelope expelled from the progenitor star several decades/centuries before explosion. The expelled envelope, moving with a velocity of $\sim$ 10–100 km s^{-1}, is expected to be caught up by the fast-moving SN ejecta several years/decades after explosion depending on the history of the mass-loss process acting in the progenitor star prior to explosion. The collision between the SN ejecta and the circumstellar envelope results in net emission in the Balmer-lines, especially in Hα. We look for signs of late-time Hα emission in older Type Ia/Ibc/IIb SNe having hydrogen-poor ejecta, via narrow-band imaging. Continuum-subtracted Hα emission has been detected for 13 point sources: 9 SN Ibc, 1 SN IIb and 3 SN Ia events. Thirty-eight SN sites were observed on at least two epochs, from which three objects (SN 1985F, SN 2005kl, SN 2012fh) showed significant temporal variation in the strength of their Hα emission in our DIAFI data. This suggests that the variable emission is probably not due to nearby H II regions unassociated with the SN, and hence is an important additional hint that ejecta-CSM interaction may take place in these systems. Moreover, we successfully detected the late-time Hα emission from the Type Ib SN 2014C, which was recently discovered as a strongly interacting SN in various (radio, infrared, optical and X-ray) bands.

Subject headings: (stars:) supernovae: general; stars: winds, outflows; (ISM:) H II regions

1. INTRODUCTION

All stars are thought to lose mass during their main-sequence and subsequent evolution. This can range from a paltry stellar wind like that from the Sun (10^{-14} $M_\odot$ yr^{-1} with speeds of hundreds of km s^{-1}) to the slow, dense winds of red giants (10^{-8}–10^{-6} $M_\odot$ yr^{-1} with speeds of tens of km s^{-1}) to brief, violent, η Carinae-like expulsions of tens of solar masses from very massive stars. At different stages of evolution, a star will undoubtedly have different modes of mass loss. Binary evolution will play a role in many cases.

While it is impossible to study in real time these different modes of mass loss in an individual star, we can do so by studying individual supernovae (SNe) for years and even decades after the explosion. The fast-moving SN shock is effectively a time machine, encountering material shed earlier in the life of the pre-supernova star.

Recent years have seen a new focus on the circumstellar media (CSM) surrounding SN sites and the interaction of supernova ejecta and shocks with CSM. Well-known CSM-interacting SN types are the Type IIP (Chugai et al. 2007), which arise in red supergiant progenitors that blow nearly steady-state winds into which the star explodes and the Type IIn (SN IIn) events, which have long been recognized to show narrow emission lines that reveal dense CSM (e.g. Filippenko 1997). In addition, the great luminosities of superluminous supernovae (SLSNe) are also thought to be powered, in some cases, by ejecta-CSM interaction (Chatzopoulos et al. 2013).

The various types of stripped-envelope SNe are also of great interest in this respect, because these events have little or no hydrogen on the progenitor at the time of explosion, but the progenitors must have once been normal hydrogen-rich stars. Such events include the Type IIb SNe, in which the hydrogen envelope has been partly expelled prior to explosion, as well as the Type Ibc, which essentially lost their H-rich envelope. The mechanism of these processes is ill-understood: it could be due to winds (Heger et al. 1997; Puls et al. 2008), episodic ejection (Smith & Owocki 2006; Pastorello et al. 2007; Shiode & Quataert 2014) or binary interactions, including common-envelope formation and ejection (see the reviews by Taam & Sandquist 2000; Smith 2014). Even some Type Ia SNe, referred to as SNe Ia-CSM, show strong Hα emission, a clear sign of CSM-interaction, in their late-phase optical spectra (Silverman et al. 2013a; Inserra et al. 2016).

The collision between the fast-moving SN ejecta and the slow-moving CSM creates the well-known double-shock pattern having the forward shock (FS) propagating into the CSM and the reverse shock **(RS)** propagating back into the ejecta (e.g. Chevalier & Fransson 2003, and references therein). The acceleration of free electrons results in strong non-thermal emission, from X-rays to radio, coming from the interaction site. Massive SN progenitors ($M \gtrsim 20$ M$_\odot$) can produce strong, fast-moving winds prior to explosion, which can create a low-density cavity around the explosion site, surrounded by a relatively dense CSM shell consisting of previously expelled (H-rich) material (e.g. Chevalier & Liang 1989). When the SN ejecta hits this dense shell, it drives a strong RS into the

[1] Department of Astronomy, University of Texas at Austin, Austin, TX, 78712, USA
[2] Konkoly Observatory, Research Centre for Astronomy and Earth Sciences, Hungarian Academy of Sciences, Konkoly Thege ut 15-17, Budapest, 1121, Hungary
[3] Department of Optics & Quantum Electronics, University of Szeged, Dom ter 9, Szeged 6720, Hungary
[4] Department of Physics and Astronomy, Trinity University, One Trinity Place, San Antonio, TX, 78212, USA
[5] Department of Astronomy, University of California at Berkeley, 501 Campbell Hall, Berkeley, CA, 94720-3411, USA

ejecta, which leads to strong X-ray radiation from the region between the RS and the ejecta-CSM interface (Nymark et al. 2006). The hard X-rays produced by the RS are mostly absorbed by the cool, dense CSM shell causing strong ionization in this medium. Subsequent recombination in this H-rich CSM shell results in emergent emission in the hydrogen Balmer-lines, mostly Hα (Chugai & Chevalier 2006). This mechanism is thought to produce intermediate-width ($FWMH \sim 2000$ - 3000 km s^{-1}) emission lines, mostly due to multiple scattering on free electrons within the shell and, to a lesser extent, bulk motion caused by the acceleration of the shell by the expanding SN ejecta at the beginning of the interaction phase. The FS propagating into the CSM can also ionize the surrounding material, which may produce additional, narrow ($FWHM \lesssim 100$ km s^{-1}) Hα emission coming from the pre-shock CSM in front of the FS. The appearance of the Balmer-emission can be especially interesting in the case of stripped-envelope SNe, since in such cases the ejecta contain only very low or negligible amount of H. Thus, the emerging Balmer-emission is a very strong indication that the ejecta have overrun the cavity and plunged into the H-rich CSM shell.

The natural expectation that the fast-moving SN ejecta must overtake the previously expelled H-rich envelope has been beautifully demonstrated in the case of the Type Ibc SN 2001em, where strong radio (Stockdale et al. 2004) and X-ray emission (Pooley & Lewin 2004) was discovered $\sim$ 3 years after explosion. These discoveries generated further interest in SN 2001em, because the radio luminosity ($L_{\rm radio} \approx 2 \times 10^{28}$ erg s^{-1} Hz^{-1} at 6 cm) as well as the X-ray luminosity ($L_{\rm X} \approx 10^{41}$ erg s^{-1}) were far above anything seen from other SNe Ibc at an age of several years. Since some fraction of SN Ibc give rise to gamma-ray bursts (GRB) where the jet is aimed in our direction, it was hypothesized by Granot & Ramirez-Ruiz (2004) that SN 2001em may have been an off-axis GRB. Pooley & Lewin (2004), however, suggested the strong interaction between the SN ejecta and a dense CSM as an alternative mechanism which also can produce the exceptionally strong X-ray luminosity as observed by *Chandra*. Indeed, the late-time optical spectrum of SN 2001em, which revealed strong Hα emission (Soderberg et al. 2004), added strong support to the ejecta-CSM interaction scenario. Chugai & Chevalier (2006) explained all the unusual late-time X-ray, radio, and optical properties, as well as the failure to resolve a possible jet via VLBI observations (Bietenholz & Bartel 2005; Schinzel et al. 2009), by suggesting that the SN ejecta had finally caught up with the cast-off hydrogen envelope of the progenitor star and that strong interaction was taking place.

A similar phenomenon is invoked in the case of PTF 11kx (Dilday et al. 2012; Silverman et al. 2013b), a Type Ia-CSM, where strong Hα emission developed $\sim$ 40d after maximum in an otherwise normal-looking Type Ia SN.

Motivated by the examples above, we started an observational survey to monitor several years-to-decades-old H-deficient SNe in order to catch signs of the starting (or ongoing) ejecta-CSM interaction. Our concept is that numerous SN Ia and/or Ibc may show detectable CSM interaction at such late phases, because their CSM shells may have reached greater distances from the explosion site than in those well-known cases when the interaction started within a few hundred days after explosion. Assuming that the H-rich envelope travels with a speed between 10 and 100 km s^{-1} (Chugai & Chevalier 2006), the interaction with the fast-moving ejecta ($v_{SN} \sim 10,000$ km s^{-1}) is expected to start roughly a decade after SN explosion if the expulsion of the envelope ended $\sim 10^4$ – 10^3 years before core collapse, depending on wind speed.

The aim of our observations is the direct detection of the Hα emission due to the collision between the H-poor SN ejecta and the surrounding H-rich CSM via imaging the SN sites through narrow-band filters centered on the (redshifted) wavelength of Hα. In Sections 2 and 3 we give details of the observations and our methodology of detecting Hα emissions. Section 4 shows our early results, which are further discussed in Section 5. Section 6 summarizes our conclusions.

2. OBSERVATIONS

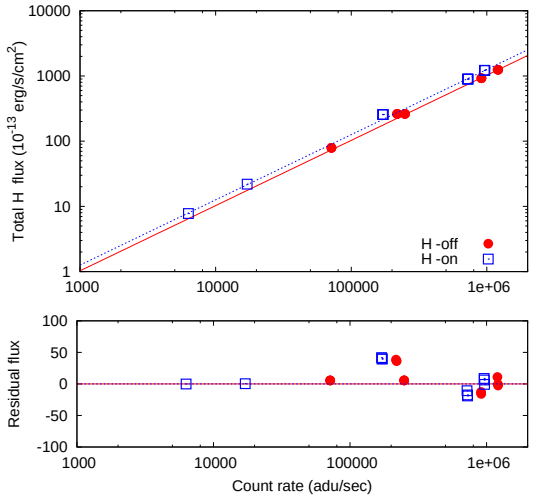

FIG. 1.— Flux calibrations for the Hα-on (blue squares) and Hα-off (red circles) filters.

We utilized the 2.7m (107") Harlan J. Smith Telescope equipped with the Direct Imaging Auxiliary Functions Instrument (DIAFI) at McDonald Observatory for conducting the imaging survey. We applied a narrow-band ($FWHM = 7$ nm) Hα filter centered on the redshift of the Virgo-cluster ($z = 0.0033$, $\lambda = 6585$ Å) and another similar filter at an off-line position ($\lambda = 6675$ Å) as a guard-band filter to measure the continuum flux near the Hα line. In the following we refer to these filters as Hα-on and Hα-off, respectively.

We have selected a subsample of the full list of 3662 known SN I (SN Ia, SN Ibc) and SN IIb discovered before 2014, based on the following selection criteria:

- declination higher than −30 deg;
- distance less than 200 Mpc.

This resulted in 747 potential candidates. These are sampled further, concentrating on the closest ($D \lesssim 30$ Mpc) events. The number of SNe in the restricted sample is 178.

Beside observability from the northern hemisphere, the reason for these selection criteria were twofold: *i*) to have the Hα line redshifted into the transmission band of the Hα-on filter, and *ii*) to be able to reach a signal-to-noise ratio of ~ 50 for L(Hα) $\sim 10^{39}$ erg s^{-1} (i.e. a signal similar to SN 2001em) within ~ 1 hour exposure time with DIAFI.

TABLE 1
THE JOURNAL OF NARROW-BAND IMAGING OBSERVATIONS WITH DIAFI

Start date	End date	No. of observed SN hosts
2014 Feb 27	2014 Feb 28	22
2014 May 03	2014 May 04	17
2014 Sep 30	2014 Oct 02	23
2015 Mar 14	2015 Mar 16	27
2015 May 20	2015 May 20	7
2015 Aug 23	2015 Aug 23	4
2016 Jun 07	2016 Jun 10	17

We started our multi-season observing campaign in 2014, using both the Hα-on and -off filters on the SNe with $D <$ 30 Mpc. Since then we have imaged 76 galaxies hosting 99 SNe, i.e. $\sim$ 55 percent of the total sample. The journal of the observations can be found in Table 1.

The Hα emission produced by SN-CSM interaction is likely to be variable in time. This offers an opportunity to distinguish between the "real" interaction-produced emission and the flux coming from the immediate vicinity of the SN site but not related to the SN blast wave (e.g. from a nearby H II cloud), because the latter sources are expected to remain roughly constant in time. Thus, instead of maximizing the number of observed SNe, we aimed at taking multiple images of those SNe that were detected as Hα emitters at significantly different epochs. This effort resulted in 38 SNe (in 32 different host galaxies) imaged at least twice, separated by a 3-month-long or longer temporal baseline.

3. METHOD

The frames taken with DIAFI were reduced and calibrated in the following way. Three frames per filter were collected for each SNe. Following standard bias-subtraction and flatfield-division, the frames obtained through the same filter were geometrically registered by applying the *IRAF*[6] task *xregister*, then they were median-combined to filter out the numerous cosmic-ray hits. The median-combined frames were then transformed to the World Coordinate System (WCS) by using the *SEXtractor*[7] and *WCSTools*[8] codes. Having the combined images properly registered in both filters, the *HOTPANTS*[9] code was applied to subtract the Hα-off frames from the Hα-on frames to produce the continuum-subtracted difference images. These images were used to look for any Hα-emitting source in the immediate vicinity of the SN as described below.

Flux calibration was performed via observing spectroscopic flux standard stars. We measured the observed count rates on the median-combined Hα-on and -off frames via aperture photometry using the *YODA*[10] ("Yet anOther object Detection Application") code (Drory 2003). The diameter of the circular aperture was chosen as d_{ap} = 15 pixels ($\sim$ 6.1 arcsec), and the fluxes within this aperture were integrated. The subtracted background flux was estimated within an annulus having inner diameter and width of 20 and 5 pixels, respectively, around each object. The correction for the atmospheric extinction was computed using the wavelength-dependent KPNO extincion function as tabulated in *IRAF*, although this was found negligible compared to other uncertainties. For the observed spectroscopic standard stars, the true Hα fluxes were calculated as the integral of their known spectral flux densities within the spectral bandpasses of the applied filters. Finally, the conversion between the observed count rates (*CR*, in ADU/s) and the true Hα fluxes for both filters have been determined by fitting the following simple relation to the data:

$$F_{H\alpha} \times 10^{13}(\mathrm{erg/s/cm^2}) = K \cdot CR(\mathrm{ADU/s}) \qquad (1)$$

Figure 1 illustrates the quality of the fit. The K scaling factors obtained this way turned out to be 1.03×10^{-3} and 1.26×10^{-3} for the Hα-off and -on filters, respectively. The uncertainties of the flux calibration, estimated from the scatter of the residual plots in the bottom panel of Figure 1, are 1.89×10^{-2} and 2.38×10^{-2} erg s^{-1} cm^{-2}, respectively.

The continuum-subtracted Hα flux at the position of every target SNe was estimated by the combination of two approaches. First, aperture photometry (using the same parameters as above) was computed with *YODA* at the SN position on the continuum-subtracted difference frames produced by *HOTPANTS*. If the total flux in the aperture exceeded the local sky level, the signal-to-noise ratio (S/N) was estimated by dividing the total flux by its uncertainty reported by *YODA*. Objects having S/N $>$ 4 were selected as detection candidates. Second, the detection candidates were examined by computing the same aperture photometry as before, but on the final, median-combined Hα-on and Hα-off frames. After transforming the measured count rates to physical fluxes (applying Equation 1), the net Hα flux was computed by subtracting the calibrated fluxes from the Hα-off frames from the fluxes measured on the Hα-on images. Again, uncertainties are estimated by adopting the values as reported by *YODA*. Only those candidates that showed S/N $>$ 4 after this step were retained as detections. This way it was possible to filter out some bogus detections, which were due to numerical artifacts on the difference images given by *HOTPANTS*.

For those objects that were observed on more than one epoch, the effect of different atmospheric transparency was corrected for in the following way: photometry of bright, unsaturated stellar sources on the Hα-off (continuum) frames were computed, and their instrumental magnitudes obtained on the 2nd night were scaled to those taken on the 1st night. Similar transformation was then computed for the Hα-on frames as well. This resulted in consistent relative photometry on the two datasets within an error of a few percent. These data were used to construct the Hα "light curves" to look for temporal variability among the detected sources (see Section 4).

4. RESULTS

We have detected (using the criterion of S/N $>$ 4) continuum-subtracted Hα emission from 27 SN sites (see Table 2). At least 14 of these detections ($\sim$ 50 percent) are clearly from diffuse Hα emitting sources, probably nearby H II areas. The others look like point sources in our DIAFI frames, but some of them appear slightly off-center with respect to the expected SN position, and thus could just be nearby compact H II clouds. Figure 2 and 3 show the collection of the positive detections.

The 3rd column of Table 2 contains the average of the redshift-independent distances taken from the NASA Extra-

[6] Image Reduction and Analysis Facility (IRAF) is distributed by the National Optical Astronomy Observatories, which are operated by the Association of Universities for Research in Astronomy, Inc., under cooperative agreement with the National Science Foundation.
[7] http://www.astromatic.net/software/sextractor
[8] http://http://tdc-www.harvard.edu/wcstools/
[9] http://www.astro.washington.edu/users/becker/v2.0/hotpants.html
[10] http://www.as.utexas.edu/~drory/yoda/index.html

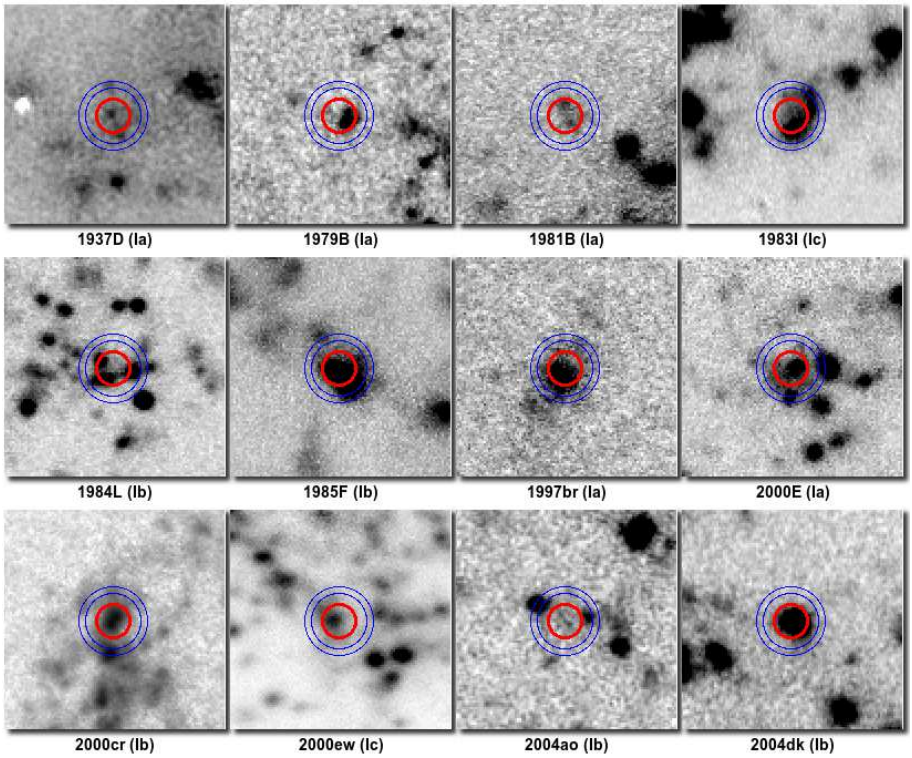

FIG. 2.— Detections of significant (S/N $>$ 4) Hα emission from the sample SN sites. Each stamp is a 0.7×0.7 arcmin^2 subset of the continuum-subtracted DIAFI frame centered on the SN position. The photometric aperture and annulus are indicated by the red and blue circles, respectively.

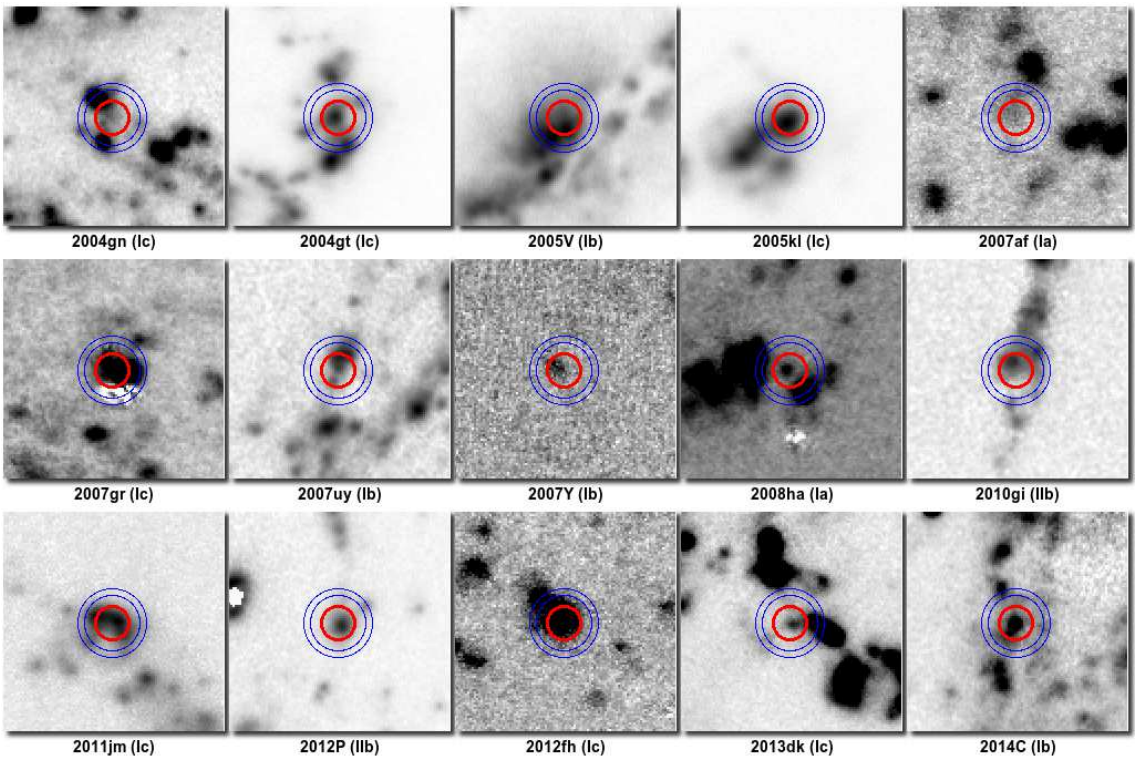

FIG. 3.— Same as Fig.2, but for additional SNe.

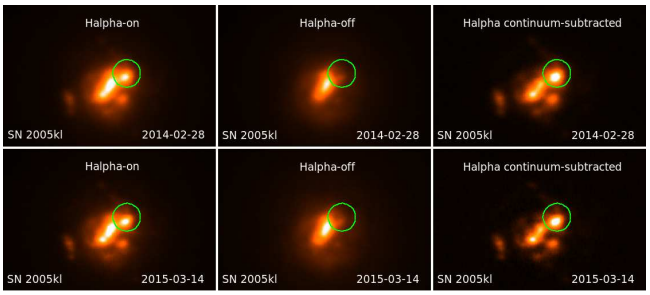

FIG. 4.— Illustration of the methodology in the case of SN 2005kl, which showed the strongest Hα flux among the detected objects. The first column shows the two frames taken through the Hα-on filter on two different epochs, the middle column contains the two Hα-off frames, while the third column displays the continuum-subtracted (i.e. Hα-on minus Hα-off) frames. The size of the frames is 1.6×1.1 arcmin^2. The position of the SN is encircled.

TABLE 2
LIST OF DETECTED OBJECTS AND THEIR Hα LUMINOSITIES (COMPUTED IN ERG S^{-1} USING THE DISTANCES IN THE 3RD COLUMN). SEE TEXT FOR DETAILS.

SN	Type	D	log L(Hα)	unc.	Remark
		(Mpc)	(cgs)	(dex)	
1937D	Ia	11.0	37.8135	0.0277	point source
1979B	Ia	17.0	37.9868	0.0070	diffuse
1981B	Ia	17.7	37.7577	0.0868	diffuse
1983I	Ic	14.0	38.6929	0.0048	diffuse
1984L	Ib	18.8	38.5064	0.0341	diffuse
1985F	Ib	7.6	38.6909	0.0121	point source
1997br	Ia	27.5	38.3376	0.0374	diffuse
2000E	Ia	23.9	38.8246	0.0231	point source
2000cr	Ib	57.6	39.5134	0.0272	point source
2000ew	Ic	17.6	39.6804	0.0647	point source
2004ao	Ib	26.9	38.0196	0.0664	diffuse
2004dk	Ib	22.8	39.1888	0.0079	point source
2004gn	Ic	14.4	38.2218	0.1629	diffuse
2004gt	Ic	21.4	40.0318	0.0109	point source
2005V	Ib	22.4	40.3510	0.0095	diffuse
2005kl	Ic	21.6	41.8452	0.0020	point source
2007Y	Ib	19.1	37.8156	0.0272	diffuse
2007af	Ia	24.3	37.8710	0.0676	diffuse
2007gr	Ic	8.2	38.4519	0.0120	diffuse
2007uy	Ib	30.0	39.2632	0.0115	diffuse
2008ha	Ia	20.0	38.2445	0.0684	point source
2010gi	IIb	10.2	38.4090	0.0635	diffuse
2011jm	Ic	22.2	39.5923	0.0030	diffuse
2012fh	Ic	16.4	38.8490	0.0008	point source
2012P	IIb	25.7	39.4327	0.0070	point source
2013dk	Ic	21.4	38.8910	0.0799	point source
2014C	Ib	14.3	38.8262	0.0527	point source

galactic Database[11] (NED). Based on these distances and the Milky Way extinction coefficient in the *R*-band from Schlafly & Finkbeiner (2011), the logarithm of the calculated Hα luminosities and their uncertainties (expressed in erg s^{-1}) are shown in the 4th and 5th columns of Table 2. The (likely underestimated) uncertainties are pure photometric errors described above and do not contain any other effects, e.g. the uncertainty of the distances or any in-host extinction.

In Figure 4 we give an example of a strong (S/N $>$ 200) detection on the continuum-subtracted image. SN 2005kl is the strongest Hα-emitting object in our sample. Its Hα luminosity, L(Hα) $\sim 7 \times 10^{41}$ erg s^{-1} (Table 2 and Figure 5), is

[11] http://ned.ipac.caltech.edu

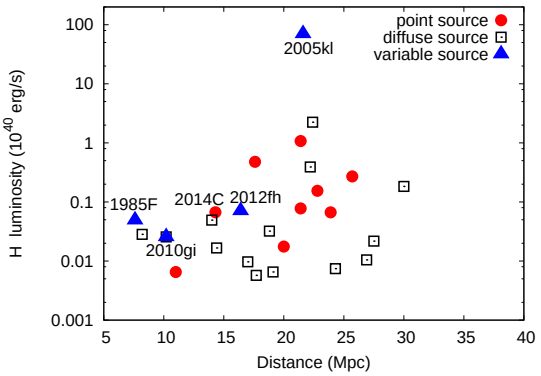

FIG. 5.— Derived Hα luminosities of the detected sources plotted against distance. Filled symbols represent the point-like sources on the DIAFI images, while open squares denote more extended (diffuse) emitting sources (see Table 2). Sources that show significant temporal variability (Figure 6) are plotted with triangles.

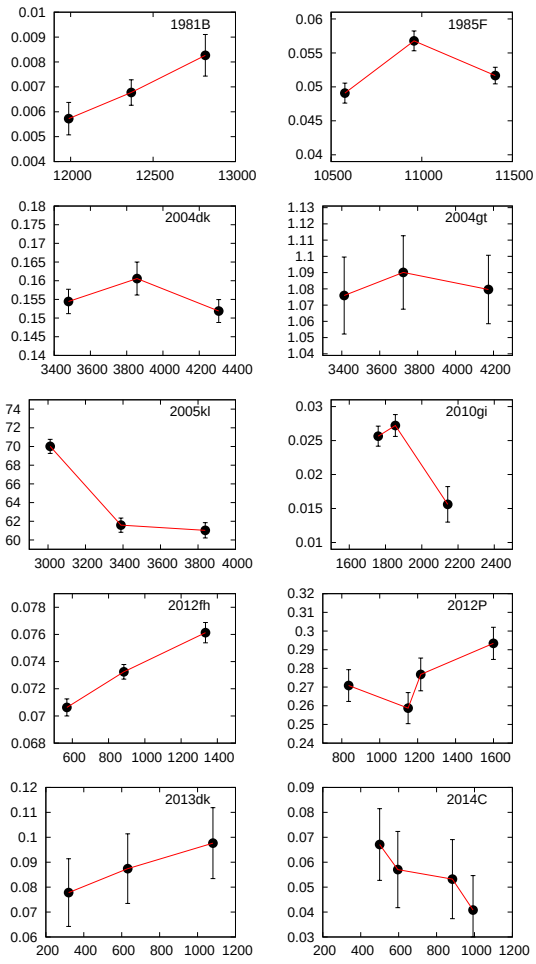

FIG. 6.— Variation of the detected Hα luminosities. Each panel shows the Hα luminosity (in 10^{40} erg s^{-1}) as a function of the rest-frame days since the SN explosion.

about an order of magnitude greater than that of the largest H II clouds (Kennicutt 1984), which strongly suggests that the detected Hα emission is (at least partly) due to SN-CSM interaction.

Figure 5 shows the plot of the derived Hα luminosities as a function of distance. It is seen that, on average, point sources

tend to be brighter than diffuse sources (the median luminosities for the two groups are 8×10^{38} erg s^{-1} and 2×10^{38} erg s^{-1}, respectively), but both types of sources can be found at all luminosity levels, except for the exceptionally bright point source SN 2005kl.

Further hints of the possible presence of ejecta-CSM interaction may be gained from the temporal variability of the detected Hα sources. SN-CSM interaction usually produces variable Hα emission on the timescale of $\sim$ 100 days (Mauerhan & Smith 2012; Fransson et al. 2014), although there are known cases, e.g. SN 1988Z, a strongly interacting Type IIn (Aretxaga et al. 1999)) showing nearly constant Hα luminosity over $\sim$ 500 days. Nevertheless, we imaged 38 SNe on at least two epochs separated by at least 90 days to detect any variability in the net Hα emission from the SN site.

In Figure 6 we plot the light curves of 10 detected Hα emitters that were observed at least three times. It is seen that 6 of them do not show any change that exceeds the uncertainties, although SN 1981B, 2013dk and 2014C exhibited continuous variation (either increase or decrease) during our observations. Flux changes exceeding the photometric errors significantly (i.e. larger than 3σ) were found in the case of SN 1985F (Ib, 3.7σ), 2005kl (Ic, 8.1σ), 2010gi (IIb, 3.3σ) and 2012fh (Ic, 5.6σ). SN 2010gi, a Type IIb SN, is a diffuse source (Figure 3) that is more affected by the changing atmospheric conditions, because the applied flux-scaling method that corrects for changing atmospheric transparency (see above) works reliably only for point sources. Thus, we do not believe that the variability detected at the position of SN 2010gi is real, and, instead, we attribute this to an instrumental effect. The other three objects are SNe-Ibc, and they are all point sources, thus, their variability is more convincing. Again, variability of the Hα line flux alone cannot be considered as proof of the ejecta-CSM interaction, but it might give additional support for this hypothesis, for example in the case of the extremely strong Hα emitter SN 2005kl, which is also a strongly variable source.

5. DISCUSSION

Even though it is difficult to prove the existence of ejecta-CSM interaction from only narrow-band imaging, without spectroscopic and/or multi-wavelength (X-ray and/or radio) observations, our data at hand strongly suggest that CSM interaction is the likely explanation for the Hα emission in at least a few of the SNe in our sample. The collision between the SN blast wave and the expelled, slowly moving H-envelope can certainly produce Hα emission in the same order of magnitude as observed, as already demonstrated by SN 2001em (Section 1).

SN 2004dk (Type Ib) is another example, where SN-CSM interaction was detected in X-rays by *XMM-Newton* shortly after explosion (Pooley 2007), and by radio observations at late phases (Stockdale et al. 2009; Wellons et al. 2012). Although Wellons et al. (2012) concluded that "it is unlikely that the shockwave is interacting with a H-rich common envelope" based on a single nebular spectum of SN 2004dk that showed only a weak, narrow, unresolved Hα emission feature attributed to ISM (Maeda et al. 2008), our solid (S/N $>$ 50) detection of a strong point source at the SN position may suggest that the blast wave has finally reached the expelled H-rich envelope. The lack of variability (Fig.6), however, does not strengthen this interpretation, thus, follow-up observations will provide important constraints for this case.

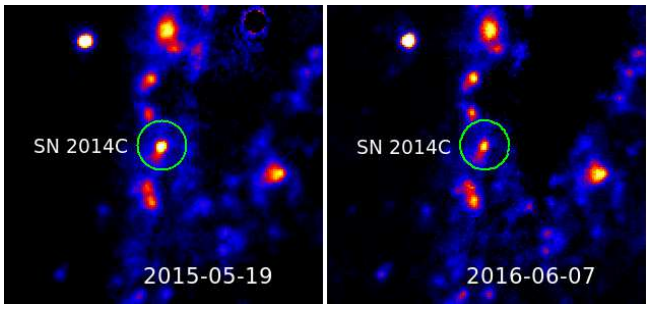

FIG. 7.— Detection of continuum-subtracted Hα emission from SN 2014C (encircled) in May 2015 (at $\sim$ 500 days after explosion) and June, 2016 (at $\sim$ 900 days). The decrease of the Hα flux between the two epochs is apparent. The size of the frames is 1×1 arcmin^2.

A more recent example occurred during the progress of our project. After emerging from solar conjunction, the Type Ib SN 2014C started to show strong Hα emission $\sim$ 110 days after explosion, even though H was absent from its spectrum during the photospheric phase (Milisavljevic et al. 2015). Accompanied by contemporaneous strong X-ray and radio emission, this remarkable metamorphosis was explained by ejecta-CSM interaction (Margutti et al. 2016), the same mechanism for which we search.

We detected the appearance of the Hα emission from SN 2014C on our DIAFI frames taken between 2015 May and 2016 June ($\sim$ 500 and $\sim$ 900 days after explosion, respectively). Figure 7 shows the continuum-subtracted DIAFI frames obtained on 2015-05-19 and 2016-06-07 (left and right panels, respectively), with the object encircled. Its Hα luminosity (Table 2) is in agreement with the independent spectroscopic measurements given by Milisavljevic et al. (2015). This source seems to show continuously decreasing net (i.e. continuum-subtracted) Hα flux (see Figure 6), but due to the relatively large errorbars of its photometry, the detected overall flux change did not exceed 2σ during the $\sim$ 1 year baseline of our observations.

More recently, SN 2014C was also detected in mid-IR bands with the *Spitzer* Space Telescope by the SPIRITS project, as a variable point source (Tinyanont et al. 2016). Note that Tinyanont et al. (2016) observed an *increase* of the mid-IR fluxes from SN 2014C between 200 and 600 days after explosion, while our observations span only the later ($t > 500$ days) phases. The latest *Spitzer* observations from the SPIRITS project, partly published by Tinyanont et al. (2016), show a slow but continuous decline of mid-IR fluxes between $\sim$ 600 and $\sim$ 1000 days in both the 3.6μ and the 4.5μ bands, in agreement with our Hα observations.

Tinyanont et al. (2016) explained the observed re-brightening of SN 2014C in the mid-IR as due to shock heating (either radiative or collisional) of pre-existing dust around SN 2014C, which is in good agreement with the observations in other bands, including our Hα detections. This highlights the importance of simultaneous observations in non-optical bands, in order to detect additional tracers of the ejecta-CSM interaction that may discriminate between the different mechanisms producing the contemporaneous Hα emission.

The relatively low number of detected Hα-emitting point sources (13 out of 99 SNe, i.e. $\sim$ 13 percent) is more-or-less consistent with the recent estimate for the rate of the SN 2001em/2014C-like events published by Margutti et al. (2016) based on late-time re-brightening in the radio. From 41 Type Ibc SNe having radio coverage at $t > 500$ days after

explosion, Margutti et al. (2016) found 4 cases (SN 2001em, SN 2003gk, SN 2007bg and SN iPTF11qcj, $\sim$ 10 percent of the sample) when luminous radio re-brightening was observed years after core collapse. Since radio light curves are usually attributed to SN-CSM interaction, the emergence of radio fluxes at such late phases are very strong signs for the ejecta-CSM collision. Their result ($\sim$ 10 %) is consistent with our detection rate ($\sim$ 13 %) when taking into account that at least some of our detected Hα emitters could also be compact H II areas very close to the SN site, i.e. the detected emission may not be due to ejecta-CSM interaction in every case.

Variability in the detected Hα line emission can be another tracer for the SN-CSM interaction, because H II clouds are usually close to ionization/recombination equilibrium, and do not show noticeable variation in their emission line strengths. On the contrary, existing models on the ejecta-CSM interaction (e.g. Chugai & Chevalier 2006; van Marle et al. 2010) predict several forms of variability in the produced radiation. The most commonly accepted scenario is the close link between the X-rays produced by the RS and the Hα line emission coming from the H-rich dense shell in between the FS and the RS (see Section 1). Since the main source of the escaping Hα line photons are the X-rays absorbed by the shell, any kind of variation in the absorbed X-rays can imply change in the emergent Hα flux. At the beginning of the interaction the models predict a relatively quick rise ($\sim$ 500 days) of the X-ray flux (Chugai & Chevalier 2006) followed by a slower decline after the FS passed through the dense shell and the shell got accelerated by the SN ejecta piling up from behind (Chevalier & Liang 1989). The deceleration of the RS, $v_{RS} \sim t^{-1/(n-2)}$, where n is the power-law index of the density profile in the outer part of the SN ejecta, is also partly responsible for the decrease of the Hα luminosity since $L_X \sim {v_{RS}}^3$ (Chevalier & Fransson 2003; Nymark et al. 2006) and $L_{H\alpha} \sim \eta L_X M_S^{9/40}$, where $\eta \sim 0.1$ is the efficiency of converting the X-ray flux to Hα photons and M_S is the mass of the dense CSM shell (Chugai & Chevalier 2006). In addition, at later phases the shell gets diluted by expansion, reducing the X-ray optical depth, which causes further decrease in the produced Hα radiation.

In Figure 6 there are examples for increasing (e.g. SN 1981B, 2012fh) as well as decreasing (SN 2005kl, SN 2014C) Hα luminosities. In the simple interaction scenario described above, the increasing Hα fluxes might be connected with an early-phase, still strengthening ejecta-CSM interaction, while the declining Hα fluxes could be explained by a more evolved interaction. The possibility for the developing ejecta-CSM interaction around the Type Ia SN 1981B, as suggested by the persistent (even though not statistically significant) increase in its Hα luminosity, is especially interesting, since is the only SN Ia in our sample that shows such a phenomenon. Since the baseline of our survey is still less than 1000 days, and we have only a few measured points for each SNe, it is premature to draw any definite conclusion on such details. Future observations will be useful to decide whether these SNe are indeed subject to ejecta-CSM interaction.

6. CONCLUSIONS

Our narrow-band imaging survey of old, H-deficient (Type Ibc, Ia and IIb) SNe through Hα filters resulted in the following:

- detection of continuum-subtracted Hα emission from 27 SNe sites (see Table 2), 13 of which are point sources at our resolution;
- detection of significant variation (exceeding 3σ) of the Hα emission from 3 SNe: SN 1985F, SN 2005kl, SN 2012fh (all SN Ibc and point sources). SN 2010gi, a diffuse source around a SN IIb, also shows some sort of variability, but its reality is more uncertain;
- a strong, variable Hα emitter, SN 2005kl (SN Ic), for which the Hα luminosity exceeds that of the typical H II regions by an order of magnitude;
- detection of Hα emission from the known late-time interacting SN 2004dk and SN 2014C;
- possible variation in the Hα emission from SN 1981B (Ia), SN 2012P (IIb), SN 2013dk (Ic) and SN 2014C (Ib).

We conclude that in the case of the three variable Hα emitters, i.e. SN 1985F, SN 2005kl and SN 2012fh, the source of the net Hα emission is likely the ongoing ejecta-CSM interaction. The robustness of our methodology is demonstrated by the successful detection of the well-known interacting SN 2004dk and SN 2014C. The number of the detected point-source Hα emitters, 13 out of 99 SNe, is consistent with the recently estimated rate ($\sim$ 10 percent) of such events (Margutti et al. 2016).

In addition to continuing our narrow-band **imaging** for all nearby Type I SNe, we plan to obtain spectroscopic and multi-wavelength data, from radio to X-ray bands, for the SNe listed in Table 2 to confirm and characterize the ejecta-CSM interaction. We are also investigating the archival radio and X-ray coverage of these SNe (Pooley et al., in prep).

This work was supported in part by the following grants: NSF Fellowship AST-1302771 (JMS), NSF Grant AST-1109881 (JCW), NKFIH/OTKA grants PD-112325 (TS) and NN-107637 (JV) of the Hungarian National Research, Development and Innovation Office. We acknowledge the helpful assistance of the McDonald Observatory staff during our observing runs. This research has made use of NASA's Astrophysics Data System Service operated by the Smithsonian Astrophysical Observatory (SAO), and the NASA/IPAC Extragalactic Database (NED) which is operated by the Jet Propulsion Laboratory, California Institute of Technology, under contract with the National Aeronautics and Space Administration.

Facilities: McDonald Observatory: 2.7m (DIAFI)

Software: IRAF, WCStools, HOTPANTS, SExtractor, YODA

REFERENCES

Aretxaga, I., Benetti, S., Terlevich, R. J., et al. 1999, MNRAS, 309, 343
Bietenholz, M. F., & Bartel, N. 2005, ApJ, 625, L99
Chatzopoulos, E., Wheeler, J. C., Vinko, J., Horvath, Z. L., & Nagy, A. 2013, ApJ, 773, 76

Chevalier, R. A., & Fransson, C. 2003, Supernovae and Gamma-Ray Bursters, 598, 171
Chevalier, R. A., & Liang, E. P. 1989, ApJ, 344, 332
Chugai, N. N., & Chevalier, R. A. 2006, ApJ, 641, 1051
Chugai, N. N., Chevalier, R. A., & Utrobin, V. P. 2007, ApJ, 662, 1136
Dilday, B., Howell, D. A., Cenko, S. B., et al. 2012, Science, 337, 942
Drory, N. 2003, A&A, 397, 371
Filippenko, A. V. 1997, ARA&A, 35, 309
Fransson, C., Ergon, M., Challis, P. J., et al. 2014, ApJ, 797, 118
Granot, J., & Ramirez-Ruiz, E. 2004, ApJ, 609, L9
Heger, A., Jeannin, L., Langer, N., & Baraffe, I. 1997, A&A, 327, 224
Inserra, C., Fraser, M., Smartt, S. J., et al. 2016, MNRAS, 459, 2721
Kennicutt, R. C., Jr. 1984, ApJ, 287, 116
Maeda, K., Kawabata, K., Mazzali, P. A., et al. 2008, Science, 319, 1220
Mauerhan, J., & Smith, N. 2012, MNRAS, 424, 2659
Margutti, R., Kamble, A., Milisavljevic, D., et al. 2016, arXiv:1601.06806
Milisavljevic, D., Margutti, R., Kamble, A., et al. 2015, ApJ, 815, 120
Nymark, T. K., Fransson, C., & Kozma, C. 2006, A&A, 449, 171
Pastorello, A., et al. 2007, Nature, 447, 829
Pooley, D., & Lewin, W. H. G. 2004, IAU Circ., 8323, 2
Pooley, D. 2007, in Supernova 1987A: 20 Years After: Supernovae and Gamma-Ray Bursters, ed. S. Immler, K. Weiler, & R. McCray, volume 937 of American Institute of Physics Conference Series, 381
Puls, J., Vink, J. S., & Najarro, F. 2008, A&A Rev., 16, 209
Schinzel, F. K., Taylor, G. B., Stockdale, C. J., Granot, J., & Ramirez-Ruiz, E. 2009, ApJ, 691, 1380
Schlafly, E. F., & Finkbeiner, D. P. 2011, ApJ, 737, 103
Shiode, J. H., & Quataert, E. 2014, ApJ, 780, 96
Silverman, J., et al. 2013a, ApJS, 207, 3
Silverman, J., et al. 2013b, ApJ, 772, 125
Smith, N., & Owocki, S. P. 2006, ApJ, 645, L45
Smith, N. 2014, ARA&A, 52, 487
Soderberg, A. M., Gal-Yam, A., & Kulkarni, S. R. 2004, GRB Coordinates Network, 2586, 1
Stockdale, C. J., et al. 2004, IAU Circ., 8282, 2
Stockdale, C. J., Heim, M. S., Vandrevala, C. M., et al. 2009, IAU Circ., 1714, 1
Taam, R. E., & Sandquist, E. L. 2000, ARA&A, 38, 113
Tinyanont, S., Kasliwal, M. M., Fox, O. D., et al. 2016, ApJ, 833, 231
van Marle, A. J., Smith, N., Owocki, S. P., & van Veelen, B. 2010, MNRAS, 407, 2305
Wellons, S., Soderberg, A. M., & Chevalier, R. A. 2012, ApJ, 752, 17